Radial-orbit instability in modified Newtonian dynamics

Carlo Nipoti,[1]* Luca Ciotti[1] and Pasquale Londrillo[2]

[1]*Astronomy Department, University of Bologna, via Ranzani 1, I-40127 Bologna, Italy*
[2]*INAF-Bologna Astronomical Observatory, via Ranzani 1, I-40127 Bologna, Italy*

ABSTRACT

The stability of radially anisotropic spherical stellar systems in modified Newtonian dynamics (MOND) is explored by means of numerical simulations performed with the *N*-body code N-MODY. We find that Osipkov–Merritt MOND models require for stability larger minimum anisotropy radii than equivalent Newtonian systems (ENSs) with the dark matter, and also than purely baryonic Newtonian models with the same density profile. The maximum value for stability of the Fridman–Polyachenko–Shukhman parameter in MOND models is lower than in ENSs, but higher than in Newtonian models with no dark matter. We conclude that MOND systems are substantially more prone to radial-orbit instability than ENSs with dark matter, while they are able to support a larger amount of kinetic energy stored in radial orbits than purely baryonic Newtonian systems. An explanation of these results is attempted and their relevance to the MOND interpretation of the observed kinematics of globular clusters, dwarf spheroidal and elliptical galaxies is briefly discussed.

Key words: gravitation – instabilities – globular clusters: general – galaxies: kinematics and dynamics – dark matter.

1 INTRODUCTION

Modified Newtonian dynamics (MOND) was originally proposed by Milgrom (1983) to explain the rotation curves of disc galaxies without invoking the presence of dark matter (DM) and, over the years, it has been successful at reproducing the observed kinematics of several galaxies (e.g. Sanders & McGaugh 2002; Sanders & Noordermeer 2007; Swaters, Sanders & McGaugh 2010, and references therein). However, to some extent, the MOND and DM interpretations of the kinematics of galaxies can be degenerate. For instance, a MOND rotation curve can also be described in the Newtonian gravity by invoking a DM halo such that the total gravitational field is the same as the MOND one. More generally, given a MOND system, it is possible to construct the *equivalent Newtonian system* (ENS), that is, the Newtonian system with the DM in which the visible matter has the same phase-space distribution as in the MOND system (Milgrom 1986, 2001; Nipoti et al. 2007b; Nipoti, Londrillo & Ciotti 2007c; Nipoti et al. 2008). It should be noted, however, that the physical viability of the ENS is not guaranteed, as for some configurations the density of the associate DM halo turns out to be negative (Milgrom 1986). Though a MOND system and its ENS are, by construction, indistinguishable from a *kinematic* point of view (for instance, as far as the rotation curve[1] or the velocity

dispersion profile are concerned), in general they are not identical from a *dynamical* point of view: for instance, two-body relaxation, dynamical friction and galaxy merging act differently in the two cases (Ciotti & Binney 2004; Nipoti et al. 2007c, 2008).

As already recognized, MOND systems and ENSs might differ substantially also in terms of stability. As one of the original motivations for invoking DM haloes in disc galaxies was that purely baryonic Newtonian discs are prone to bar-like instability (Ostriker & Peebles 1973), it is not surprising that the study of dynamical stability in MOND has focused mainly on discs (Milgrom 1989; Christodoulou 1991; Brada & Milgrom 1999). Here we consider instead the so-called radial-orbit instability, which is relevant to pressure-supported stellar systems. As is well known, in the context of Newtonian gravity, the amount of radial orbits in stellar systems is limited not only by the requirement of phase-space consistency (i.e. positivity of the distribution function; see e.g. Ciotti & Pellegrini 1992; An & Evans 2006; Ciotti & Morganti 2009, 2010a,b), but also by the fact that very radially anisotropic spherical systems are unstable (Henon 1973; Polyachenko & Shukhman 1981; Fridman & Polyachenko 1984; Merritt & Aguilar 1985; Barnes, Hut & Goodman 1986; May & Binney 1986; Palmer & Papaloizou 1987; Dejonghe & Merritt 1988; Saha 1991; Weinberg 1991; Bertin et al. 1994; Hjorth 1994; Meza & Zamorano 1997; Trenti & Bertin 2006; Barnes, Lanzel & Williams 2009). In Newtonian gravity, DM haloes tend to have a stabilizing effect against radial-orbit instability (Stiavelli & Sparke 1991; Meza & Zamorano 1998; Nipoti, Londrillo & Ciotti 2002), which suggests that MOND systems might be more prone to this kind of instability than their ENSs. If confirmed, this could provide a discriminant between

*E-mail: carlo.nipoti@unibo.it

[1] The MOND rotation curve of a disc galaxy can be always reproduced with a *spherical* DM halo and Newtonian gravity. However, the vertical kinematics differ in the two cases (Nipoti et al. 2007b), because the DM halo of the ENS of a disc galaxy is non-spherical.

the two theories when interpreting the velocity dispersion profiles in pressure-supported stellar systems. For these reasons, in this work, we use N-body simulations to explore the stability of radially anisotropic MOND spherical systems and, for comparison, of their ENSs and of purely baryonic Newtonian systems with the same density distributions and anisotropy profiles.

This paper is organized as follows. In Section 2, the galaxy models used in the simulations are described. Their phase-space consistency is discussed in Section 2.1 and their stability in Section 3. Section 4 concludes.

2 GALAXY MODELS

We consider MOND as modified gravity in the non-relativistic formulation[2] of Bekenstein & Milgrom (1984), in which the Poisson equation $\nabla^2\phi^N = 4\pi G\rho$ is replaced by

$$\nabla \cdot \left[\mu \left(\frac{\|\nabla\phi\|}{a_0} \right) \nabla\phi \right] = 4\pi G\rho, \quad (1)$$

where $\|\ldots\|$ is the standard Euclidean norm, ϕ is the MOND gravitational potential, $a_0 \simeq 1.2 \times 10^{-10}\,\mathrm{m\,s^{-2}}$ is the characteristic acceleration and μ is the so-called interpolating function [in this work, we adopt $\mu(y) = y/\sqrt{1+y^2}$; Milgrom 1983]. The MOND gravitational acceleration is $\boldsymbol{g} = -\nabla\phi$, just as the Newtonian acceleration is $\boldsymbol{g}^N = -\nabla\phi^N$. For a system of finite mass, $\nabla\phi \to 0$ as $\|\boldsymbol{x}\| \to \infty$, where $\boldsymbol{x}$ is the position vector.

As is well known, from the Poisson equation and equation (1) it follows that the MOND and Newtonian gravitational accelerations are related by $\mu(g/a_0)\,\boldsymbol{g} = \boldsymbol{g}^N + \boldsymbol{S}$, where $g \equiv \|\boldsymbol{g}\|$ and $\boldsymbol{S}$ is a solenoidal field dependent on the specific ρ considered. Since in general $\boldsymbol{S} \neq 0$, and its expression is unknown a priori, standard Poisson solvers cannot be used to develop MOND N-body codes, in which equation (1) must be solved at each time-step (see Brada & Milgrom 1999; Ciotti, Londrillo & Nipoti 2006; Tiret & Combes 2007). In this work, we use our original MOND N-body code N-MODY (Nipoti et al. 2007a; Londrillo & Nipoti 2009; see Section 3.1).

The initial conditions of the simulations are N-body realizations of galaxy models with the stellar component described by a spherical γ-model (Dehnen 1993; Tremaine et al. 1994) with the density distribution

$$\rho_*(r) = \frac{3-\gamma}{4\pi} \frac{M_* r_*}{r^\gamma (r_* + r)^{4-\gamma}}, \quad (2)$$

where M_* is the total stellar mass, r_* is the scale radius and γ is the negative of the inner logarithmic density slope ($0 \leq \gamma < 3$). For simplicity, we restrict to the cases $\gamma = 0$ and 1 (Hernquist 1990); we recall that for $\gamma \neq 2$ the Newtonian potential is

$$\phi_*^N(r) = \frac{GM_*}{r_*(2-\gamma)} \left[\left(\frac{r}{r_* + r} \right)^{2-\gamma} - 1 \right]. \quad (3)$$

For these models, the MOND potential, required to distribute the particles in the velocity space, is easily calculated from the Newtonian one, as in spherical symmetry $\boldsymbol{S} = 0$. The ENS associated with a model of the stellar density ρ_* and MOND potential ϕ has the *total* density $\nabla^2\phi(r)/4\pi G$. However, the resulting DM halo density (obtained after the subtraction of ρ_*), in principle, may be negative or have a non-monotonic radial trend. Fortunately, it can be proved

that the DM haloes of the ENS derived from the spherical $\gamma = 0$ and $\gamma = 1$ models are everywhere positive. Instead, the possible non-monotonicity of the DM density distribution makes the consistency of the halo a non-trivial request, as we will discuss in Section 2.1 (see also Ciotti, Morganti & de Zeeuw 2009).

In order to impose a tunable amount of radial anisotropy on the initial conditions, we adopt the widely used Osipkov–Merritt (OM) parametrization (Osipkov 1979; Merritt 1985), in which the stellar distribution function depends on the energy and angular momentum per unit mass through the variable $Q \equiv \mathcal{E} - J^2/2r_a^2$, where $\mathcal{E} = \Psi - v^2/2$ is the relative energy, $v = \|\boldsymbol{v}\|$ is the velocity modulus, $\Psi = -\phi$ is the relative potential, J is the angular momentum modulus per unit mass and r_a is the so-called anisotropy radius. The anisotropy parameter (e.g. Binney & Tremaine 2008) is $\beta(r) = r^2/(r_a^2 + r^2)$: for $r \gg r_a$ the velocity dispersion tensor is radially anisotropic, while for $r \ll r_a$ the tensor is nearly isotropic. In the limit $r_a \to \infty$, $Q = \mathcal{E}$ and the velocity dispersion tensor becomes globally isotropic.

In the purely baryonic Newtonian models, the distribution function can be written as

$$f_N(Q) = \frac{1}{\sqrt{8}\pi^2} \frac{\mathrm{d}}{\mathrm{d}Q} \int_0^Q \frac{\mathrm{d}\varrho_*}{\mathrm{d}\Psi_*^N} \frac{\mathrm{d}\Psi_*^N}{\sqrt{Q - \Psi_*^N}}, \quad (4)$$

where $\Psi_*^N = -\phi_*^N$ is the Newtonian relative potential and

$$\varrho_*(r) = \left(1 + \frac{r^2}{r_a^2} \right) \rho_*(r) \quad (5)$$

is the so-called augmented density (see e.g. Binney & Tremaine 2008).

In the MOND (and in the ENS) cases, a similar formula holds, that is,

$$f_M(Q) = \frac{1}{\sqrt{8}\pi^2} \frac{\mathrm{d}}{\mathrm{d}Q} \int_{-\infty}^Q \frac{\mathrm{d}\varrho_*}{\mathrm{d}\Psi} \frac{\mathrm{d}\Psi}{\sqrt{Q - \Psi}}, \quad (6)$$

where now Ψ is the MOND relative potential that, by construction, is also the total potential of the ENS. Note that, at variance with equation (4), the lower integration limit is now $-\infty$: due to the far-field logarithmic behaviour of the MOND potential in isolated systems of finite mass, the distribution function must be positive for all values of $Q < 0$ in analogy with finite-mass Newtonian systems in a total isothermal potential, where stars of all energies are bound (e.g. Ciotti et al. 2009). Apart from a few exceptions (see Section 3.2.3), in the simulations of the ENSs, the halo is maintained 'frozen' (i.e. it acts as a fixed external potential), so its distribution function is not needed.

2.1 Consistency

As is well known, in (single- or multi-component) OM models, it is possible to determine a critical value of the anisotropy radius of each density component, r_{ac}, so that for $r_a < r_{ac}$ the models are inconsistent, that is, $f(Q) < 0$ for some admissible values of Q. A necessary condition for the consistency of OM models is $\mathrm{d}\varrho_*(r)/\mathrm{d}r \leq 0$ at all radii (Ciotti & Pellegrini 1992; Ciotti 1996, 1999; Ciotti et al. 2009). As recently proved in Ciotti & Morganti (2010a,b; see also Van Hese, Baes & Dejonghe 2011; An 2011), this condition is rigorously equivalent to the global density slope–anisotropy inequality (GDSAI), that is, to the requirement that at each radius, the negative of the logarithmic slope of the stellar density distribution cannot be less than twice the local value of the anisotropy parameter, $\gamma_*(r) \geq 2\beta(r)$. Remarkably, it is easy to show that the GDSAI *is independent of the gravity law holding the system*

---

[2] Recently, an alternative non-relativistic formulation of MOND, dubbed QUMOND, has been proposed (Milgrom 2010).

Table 1. Main properties of the studied families of models.

Family (1)	Gravity (2)	$(M_{\rm DM}/M_*)_{\rm half}$ (3)	$r_{\rm ac}/r_{\rm half}$ (4)	$r_{\rm as}/r_{\rm half}$ (5)	$\xi_{\rm s}$ (6)	$\xi_{\rm half,s}$ (7)
N_0	Newtonian	0	0.092	~0.8	~1.75	~1.34
$M_0\kappa_{10}$	MOND	0	0.092	~1.0	~2.33	~1.26
$E_0\kappa_{10}$	Newtonian	0.76	0.092	~0.5	~3.48	~1.83
$M_0\kappa_{0.01}$	MOND	0	0.092	~1.0	~2.48	~1.28
$E_0\kappa_{0.01}$	Newtonian	50.1	0.092	<0.2	>7.48	>4.06
N_1	Newtonian	0	0.053	~0.8	~1.64	~1.28
$M_1\kappa_{10}$	MOND	0	0.053	~0.8	~2.32	~1.31
$E_1\kappa_{10}$	Newtonian	0.31	0.053	~0.6	~2.70	~1.50
$M_1\kappa_{0.01}$	MOND	0	0.053	~0.9	~2.61	~1.31
$E_1\kappa_{0.01}$	Newtonian	32.7	0.053	<0.2	>6.86	>3.64

Column (1) – name of the family of models: N represent the Newtonian purely baryonic models, M represent the MOND models and E represent the ENS models. The first subscript is the value of the parameter γ identifying the stellar density profile (equation 2); the second subscript is the value of the internal acceleration ratio $\kappa \equiv GM_*/a_0 r_*^2$. Column (2) – gravity law. Column (3) – the DM-to-stellar mass ratio within the stellar half-mass radius $r_{\rm half}$ ($r_{\rm half} \simeq 3.84 r_*$ for $\gamma = 0$ and $r_{\rm half} \simeq 2.41 r_*$ for $\gamma = 1$). Column (4) – the normalized critical anisotropy radius for consistency, as determined from the GDSAI. Models with $r_{\rm a} < r_{\rm ac}$ are necessarily inconsistent. Column (5) – the normalized minimum anisotropy radius for stability. Column (6) – the maximum value for stability of twice the Fridman–Polyachenko–Shukhman parameter. Column (7) – the maximum value for stability of the radial-to-tangential kinetic energy ratio measured within $r_{\rm half}$. In Columns (5)–(7), the upper limits on $r_{\rm a}$ and lower limits on $\xi_{\rm s}$ and $\xi_{\rm half,s}$ mean that no instability has been detected in the most anisotropic case explored for that family.

together, so that it holds not only for Newtonian multicomponent systems (such as the ENSs), but also for the MOND case.[3]

We applied the GDSAI to our families of models, determining for each stellar density profile the value of $r_{\rm ac}$ (see Table 1), and the obtained limits coincide with those determined in Ciotti (1999). As these are just necessary conditions for consistency, the positivity of the distribution function must still be checked numerically for $r_{\rm a} \geq r_{\rm ac}$. We also note that from the inequality $d\varrho_*(r)/dr \leq 0$ it follows that in the case of isotropy ($r_{\rm a} = \infty$), a spherical density distribution must be necessarily monotonically decreasing for increasing r, and this imposes quite strong constraints on the DM haloes of physically admissible ENSs. If the halo has a central 'hole' (which is not unusual for ENSs; see Nipoti et al. 2007c), it can be physically realized only if its orbital distribution is tangentially biased, at least in the internal regions. In practice, this is not an issue in simulations with the frozen DM haloes, but it is an important problem when setting up initial conditions for simulations in which the DM halo is 'live' (i.e. modelled with particles; see Section 3.2.3).

3 STABILITY

We now describe the main results of the *N*-body simulations. Before, we briefly illustrate the numerical code N-MODY and the tests performed.

3.1 The numerical simulations

We ran *N*-body simulations with N-MODY, our original parallel three-dimensional particle-mesh code that can be used to follow the evolution of either MOND or Newtonian collisionless stellar

systems (Nipoti et al. 2007a; Londrillo & Nipoti 2009). In previous papers, we have already used N-MODY to demonstrate significant differences in the violent relaxation, merging and dynamical friction in MOND and Newtonian dynamics (Ciotti, Londrillo & Nipoti 2007; Nipoti et al. 2007a,c; Nipoti et al. 2008). We refer the readers to these papers and to Londrillo & Nipoti (2009) for a more detailed description of the code. In this study, the spherical grid has 64 radial nodes, 32 nodes in colatitude ϑ and 64 nodes in azimuth φ, and the total number of particles is $N_{\rm part} \simeq 8 \times 10^5$. We verified with convergence experiments that these numbers of particles and grid points exclude important discreteness effects. In particular, we re-ran some of the simulations with a grid $128 \times 64 \times 128$ and $N_{\rm part} \simeq 6.4 \times 10^6$, finding that the results are almost identical to the corresponding lower resolution cases.

In each simulation, the initial conditions consist of an *N*-body realization of the stellar distribution of an isolated equilibrium galaxy model, in which the particles are distributed in phase space with the standard rejection technique, using the numerically recovered distribution functions. In the ENS simulations, even if the DM halo is frozen, the systems are truncated exponentially at a radius $r_{\rm t}$, so that the potential well is finite. As a rule, we adopt $r_{\rm t} = 10 r_*$, but we ran some of the simulations also with $r_{\rm t} = 100 r_*$ and $1000 r_*$, finding that the stability properties of a model do not depend on the specific choice of the truncation radius.

Following Nipoti et al. (2007c), we identify each MOND initial condition by fixing a value of the dimensionless internal acceleration parameter $\kappa \equiv GM_*/a_0 r_*^2$, so M_* and r_* are not independent quantities. In physical units, introducing the quantity $M_{*,10} \equiv M_*/10^{10} \, {\rm M_\odot}$, $r_* \simeq 3.4\kappa^{-1/2}M_{*,10}^{1/2}$ kpc, the time and velocity units are $t_* \equiv \sqrt{r_*^3/GM_*} \simeq 29.7\kappa^{-3/4}M_{*,10}^{1/4}$ Myr and $v_* \equiv r_*/t_* \simeq 112\kappa^{1/4}M_{*,10}^{1/4}$ km s^{-1}, respectively. The simulations are evolved up to $100 t_{\rm dyn}$ with a time-step $\Delta t = 0.01 t_{\rm dyn}$, where $t_{\rm dyn}$ is the characteristic dynamical time of the system. In the purely

---

[3] This, however, is not true for the *sufficient conditions* for consistency (see Ciotti & Morganti 2010a,b)

baryonic Newtonian γ-models, we adopt the standard half-mass radius value

$$t_{\rm dyn} \equiv \sqrt{\frac{3\pi}{16 G \rho_{\rm half}}} = \frac{\pi t_*}{\sqrt{2}[2^{1/(3-\gamma)} - 1]^{3/2}}, \quad (7)$$

where $\rho_{\rm half} = 3M_*/8\pi r_{\rm half}^3$ is the mean stellar density inside the half-mass radius $r_{\rm half}$ (we recall that $r_{\rm half} \simeq 3.84 r_*$ for $\gamma = 0$ and $r_{\rm half} \simeq 2.41 r_*$ for $\gamma = 1$). In the corresponding MOND models (and their ENSs), $t_{\rm dyn}$ is given by the above expression multiplied by v_c^N/v_c^M, where v_c^N is the circular velocity at $r_{\rm half}$ for the purely baryonic Newtonian system and v_c^M is the same quantity for the MOND system.

Following Nipoti et al. (2002), in order to determine whether a given model is unstable, we check its departures from spherical symmetry by monitoring the evolution of its intrinsic axial ratios c/a and b/a (where a, b and c are the longest, intermediate and shortest axes, respectively, of the inertia ellipsoid of the stellar distribution). As preliminary tests we ran simulations in which the initial conditions are purely baryonic Newtonian systems, MOND systems and ENSs with isotropic distribution functions. We found that numerical uncertainties (due to the finite number of particles) on c/a and b/a never exceed 1 per cent over $100 t_{\rm dyn}$ of the evolution of these stable isotropic models. As a consequence, we define *unstable* the models for which the axial ratio $(c/a)_{\rm fin}$ after $100 t_{\rm dyn}$ is smaller than a fiducial threshold value $c/a = 0.99$. In the simulations, the onset of the instability is just due to numerical noise produced by discreteness effects in the initial conditions. As expected, we found that an exact determination of the stability threshold for a given family of models is not straightforward: while for strongly anisotropic initial conditions the onset of the instability is apparent and the numerical models settle down into a final equilibrium configuration in a few dynamical times, for nearly stable initial conditions, the instability can be characterized by very slow growth rates and its effects become evident even after tens of $t_{\rm dyn}$.

3.2 Results

For a given initial stellar density profile (i.e. $\gamma = 0$ or 1 in equation 2), we explored, besides the purely baryonic Newtonian case (models N_0 and N_1 in Table 1), two families of MOND systems (and the corresponding families of ENSs) characterized by the values of the acceleration ratio $\kappa = 0.01$ and 10 (see Table 1 for a summary). The cases with $\kappa = 0.01$ correspond to low-acceleration systems with internal accelerations everywhere much lower than a_0, in the so-called deep-MOND regime. Their associated ENSs are therefore totally DM-dominated systems (Table 1, Column 3). On the other hand, the $\kappa = 10$ cases are systems with relatively high accelerations within $r_{\rm half}$, corresponding in the Newtonian context to systems dominated by baryons in the central regions and by the DM only at $r \gtrsim r_{\rm half}$ (Table 1, Column 3). The lower and upper panels of Fig. 1 show the baryonic and DM initial density profiles of the ENSs corresponding to the $\kappa = 0.01$ and $\kappa = 10$ MOND systems, respectively, for the two explored values of γ. As can be seen, the associated DM haloes do not show a central hole and so, at least from this point of view, they are not unrealistic (see Section 2.1).
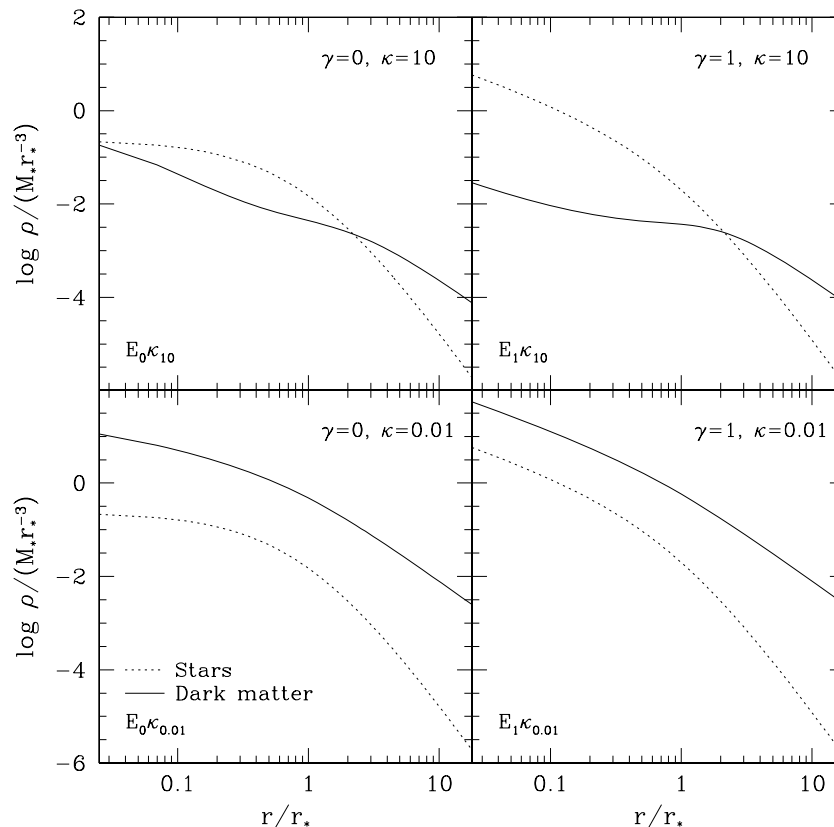

Figure 1. Stellar (deshed curves) and DM (solid curves) density profiles of ENSs corresponding to spherical MOND $\gamma = 0$ (left-hand column) and $\gamma = 1$ (right-hand column) models, for two different values of the dimensionless acceleration ratio $\kappa = GM_*/a_0 r_*^2$.
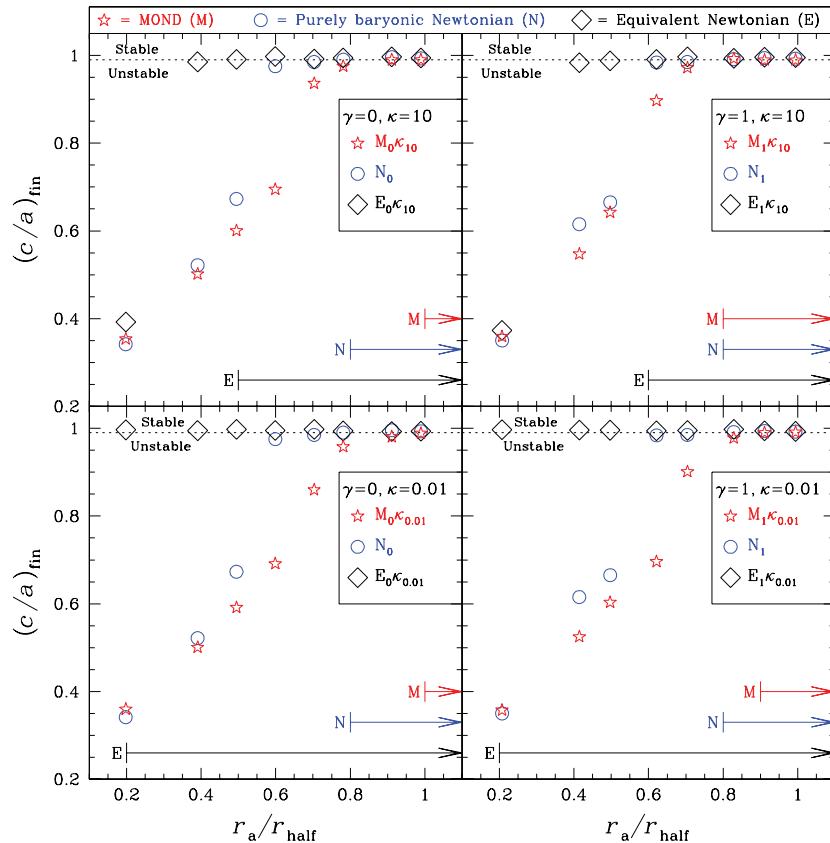
Figure 2. Final axial ratio $(c/a)_{fin}$ as a function of the initial anisotropy radius normalized to the half-mass radius for MOND systems (stars), purely baryonic Newtonian systems (circles) and ENSs (squares) with different values of γ and κ. In each panel, the horizontal dashed line marks the fiducial threshold value for stability, $(c/a)_{fin} = 0.99$; the arrows indicate the range of r_a/r_{half} corresponding to stable models.

3.2.1 Minimum value for the stability of the anisotropy radius

For each family of models, we have a set of eight simulations, in which the initial conditions differ only in the value of the normalized anisotropy radius r_a/r_{half}. This is apparent in Fig. 2, where we plot the final axial ratio $(c/a)_{fin}$ versus the initial value of r_a/r_{half} for all the explored models of the 10 families. The stability properties of the models can be inferred directly from Fig. 2: it is clear that the value of r_a at which instability appears is largest for MOND models, smallest for the corresponding ENSs and intermediate for purely baryonic Newtonian systems. Because of the very nature of the radial-orbit instability (very slow growth rates for marginally unstable systems), a precise determination of the value of the minimum anisotropy radius for stability, r_{as}, is difficult. What can be estimated robustly with N-body simulations is a fiducial value of r_{as} separating apparently unstable systems from *bona fide* stable systems. Adopting as a fiducial threshold for stability $(c/a)_{fin} = 0.99$ (horizontal dashed line in each panel of Fig. 2), we estimate for each family of models the minimum anisotropy radius for stability, r_{as}, which is reported (in units of r_{half}) in Table 1.

As expected, the differences in the stability limit between MOND systems and ENSs are more evident in systems with lower values of the acceleration ratio κ (or, from a Newtonian point of view, for more DM dominated systems). For instance, if we consider $\gamma = 0$ models with $\kappa = 0.01$, which are representative of low-surface-density systems with flat inner stellar density profiles (such as dwarf spheroidal galaxies), we find $r_{as}/r_{half} \sim 1$ for the MOND system and $r_{as}/r_{half} < 0.2$ for the ENS; very similar results are obtained for the

more peaked Hernquist $\gamma = 1$ models. Unsurprisingly, Newtonian models with the DM halo are less subject to the radial-orbit instability than the purely baryonic Newtonian models.

Thus, from this first analysis, we conclude that, when using r_a/r_{half} as an indicator of the amount of admissible radial orbits, MOND systems are more prone to radial-orbit instability than their associated ENSs, and also than corresponding purely baryonic Newtonian models. However, as we will see in the next section, the comparison between the MOND and the associated purely baryonic Newtonian families is subtle: the fact that the latter typically admit smaller r_a/r_{half} values does not imply that (globally) they can sustain more radial kinetic energy.

3.2.2 Maximum value for the stability of the ξ parameter

Stability limitations expressed in terms of r_a are particularly relevant to observational works, as r_a enters directly into the Jeans equations that are routinely used to fit the velocity dispersion profiles of stellar systems. However, from a deeper point of view, the value of r_a (loosely speaking, the radius outside which orbits are mainly radial) is not a robust measure of the fraction of the kinetic energy that is stored in radial orbits, which, at least in the Newtonian context, is believed to be the main indicator of the tendency to develop radial-orbit instability. More specifically, it has been argued (Polyachenko & Shukhman 1981; Fridman & Polyachenko 1984) that a proper criterion for stability for Newtonian self-gravitating systems can be expressed in terms of the global anisotropy parameter $\xi \equiv 2T_r/T_t$,
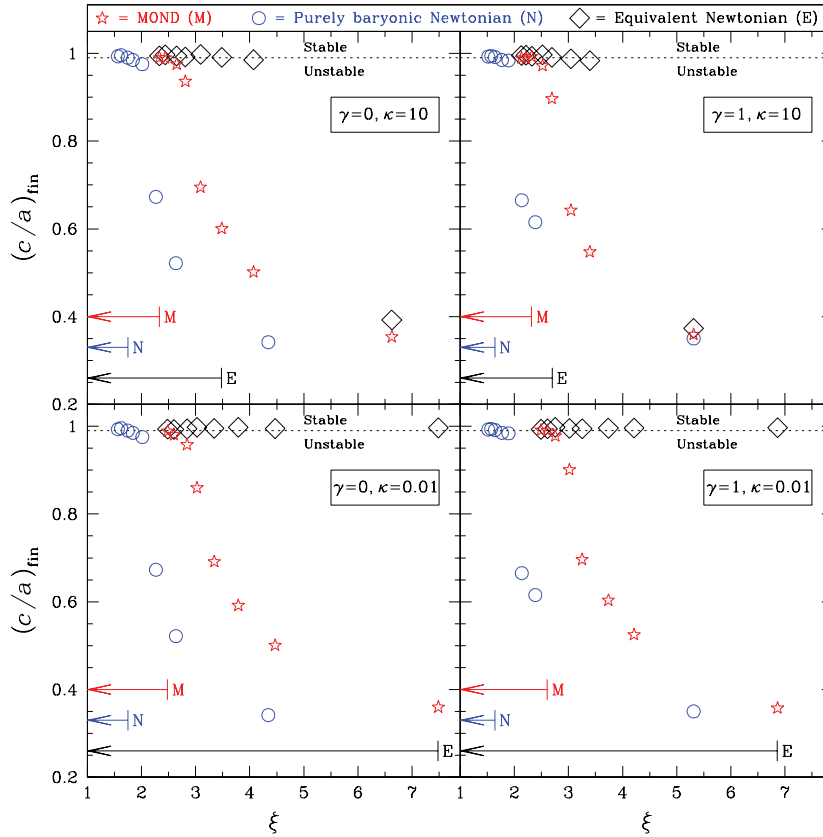
Figure 3. Final axial ratio $(c/a)_{\text{fin}}$ as a function of the Fridman–Polyachenko–Shukhman parameter ξ, for the same models as in Fig. 2. The arrows indicate the range of ξ corresponding to stable models.

where T_r and $T_t \equiv T_\vartheta + T_\varphi$ are the radial and tangential components of the kinetic energy tensor, respectively. Global isotropy corresponds to a value of the Fridman–Polyachenko–Shukhman parameter $\xi = 1$. Indications exist that there is a critical value ξ_s such that only systems with $\xi \leq \xi_s$ are stable and it is widely accepted that $\xi_s \approx 1.7 \pm 0.25$, relatively independent of the specific density distribution.

A priori, we do not have reasons to expect that ξ can be used as a stability indicator also in MOND. In any case, by definition, ξ_s measures how much radial anisotropy can be supported by a stable system, so it is interesting to discuss the stability properties of our MOND systems, purely baryonic Newtonian systems and ENSs in terms of ξ. The values of ξ_s for the families of models studied in this work are reported in Table 1, and in Fig. 3 we show all the models in the $(c/a)_{\text{fin}}$–ξ plane to be compared with the analogous Fig. 2.

For the purely baryonic Newtonian models, the interpretation of these numbers is straightforward: we find $\xi_s \sim 1.6$–1.8, in agreement with the standard criterion and with previous numerical studies (see e.g. Nipoti et al. 2002). For the MOND models, we find $2.3 \lesssim \xi_s \lesssim 2.6$, with ξ_s depending on both the stellar density profile and the acceleration ratio κ. These values are substantially higher than those found for the corresponding purely baryonic Newtonian models, indicating that, for a given density distribution, MOND systems can sustain more radial kinetic energy than Newtonian systems without the DM. This is not in contrast with the findings reported in the previous section, that is, MOND models have larger r_{as} than purely baryonic Newtonian models. In fact, for a fixed density profile and r_a value, a MOND model has higher ξ than a purely baryonic Newtonian model, because more kinetic energy is stored in the outer parts, where orbits are radially biased and the gravitational field of MOND systems is stronger.[4] Apparently, this effect compensates for the larger values of admissible r_a. Instead, the ENSs are again found able to sustain systematically higher values of ξ_s than the corresponding families of MOND systems, and this clearly indicates that MOND systems are more subject to radial-orbit instability than Newtonian models with the DM and identical total gravitational field.

In general, for both MOND systems and ENSs, we find a substantial spread in the values of ξ_s, supporting the expectation that a 'universal' value of ξ_s does not exist for these systems (for Newtonian models with the DM, extended versions of the stability criterion have been proposed; Polyachenko 1987; Stiavelli & Sparke 1991). The data in Table 1 suggest that in MOND systems, and even more in the ENSs, ξ_s increases (i.e. relatively more kinetic energy can be stored in radial orbits) for decreasing κ. While for the ENSs this trend can be explained because in the limit $\kappa \to 0$ the stars become just tracers, it is tempting to speculate that in MOND this behaviour can be interpreted as a manifestation of the less-mixing nature of MOND with respect to Newtonian gravity. This interpretation is supported by the well-established numerical finding that the phase mixing (Ciotti et al. 2007) and violent relaxation (Nipoti et al.

---

[4] Note that by construction a MOND model and its ENS, with an identical value of r_a, have the same value of ξ.

2007a) in MOND systems take longer (in units of dynamical times) than in the Newtonian case. Very qualitatively, the deep-MOND force between particles behaves like $1/r$, that is, it is nearer to the harmonic oscillator force than the $1/r^2$ force, and it is easy to show that a system in which particles interact with the harmonic oscillator force, no mixing or instabilities are possible, as each particle moves independently of the others (Lynden-Bell & Lynden-Bell 1999). Curiously, even though MOND forces in a system of particles are non-additive, a similar trend towards longer relaxation times has also been found recently in shell models interacting with additive $1/r^\alpha$ forces (Di Cintio & Ciotti 2011) and the phase-space evolution of the case with $1/r$ forces is strikingly similar to the deep-MOND collapses presented in Ciotti et al. (2007).

The fact that ξ in MOND is strongly affected by the properties of the system at large radii suggests to consider as a possible stability indicator the quantity ξ_{half}, defined as twice the ratio of the radial to tangential kinetic energy within r_{half}: the maximum values for stability, $\xi_{half,s}$, for our families of models are reported in the last column of Table 1. Remarkably, all our MOND and purely baryonic Newtonian families have $\xi_{half,s} \sim 1.3$, while the ENSs have $\xi_{half,s} \gtrsim 1.5$ for $\kappa = 10$ and $\xi_{half,s} \gtrsim 3.6$ for $\kappa = 0.01$, which leads us to speculate that *a limit on the amount of the radial orbits within the half-mass radius might be used as an empirical stability criterion for MOND stellar systems, valid from the Newtonian to the deep-MOND regime, that is, independent of the value of the internal acceleration relative to* a_0. This result is reminiscent of that of Trenti & Bertin (2006), who found that an almost isotropic core can stabilize Newtonian self-gravitating systems with very strong global radial anisotropy.

3.2.3 Simulations of ENSs with live DM haloes

The results on the stability of the ENSs might be affected to some extent by our assumption of a frozen DM halo, because it is possible that an ENS with a live DM halo has different stability properties (see Stiavelli & Sparke 1991). In order to assess to what extent our results are affected by the assumption of frozen DM haloes, we re-ran the ENS simulations of the family $E_0\kappa_{10}$ with live DM haloes. For technical reasons, we ran these live-halo simulations with our FVFPS tree code (Fortran Version of a Fast Poisson Solver; Londrillo, Nipoti & Ciotti 2003; Nipoti, Londrillo & Ciotti 2003), which was already tested against N-MODY in Nipoti et al. (2007c). As an additional test, we re-ran with FVFPS all the purely baryonic Newtonian simulations of the family N_0, finding excellent agreement with those run with N-MODY. In the live-halo simulations of the models of the family $E_0\kappa_{10}$, we used $\simeq 8 \times 10^5$ particles for the stellar component and $\simeq 1.3 \times 10^6$ particles for the halo, which has mass $\simeq 1.6M_*$ for the adopted truncation radius $r_t = 10r_*$. We verified numerically that for these two-component $E_0\kappa_{10}$ models the halo density distribution, which is monotonically decreasing (see Fig. 1) and thus satisfies the necessary condition for consistency (see Section 2.1), can be generated by a positive isotropic distribution function, which we used to distribute the DM particles in phase space with the standard rejection technique.

The final axial ratios of the live-halo simulations (hexagons in Fig. 4) are not significantly different from those of the corresponding frozen-halo simulations (squares in Fig. 4). It follows that the stability properties of the $E_0\kappa_{10}$ family of models do not depend on whether the halo is modelled with particles or it is a fixed potential: in particular, the values of the minimum anisotropy radius r_{as} (and then of the maximum Fridman–Polyachenko–Shukhman
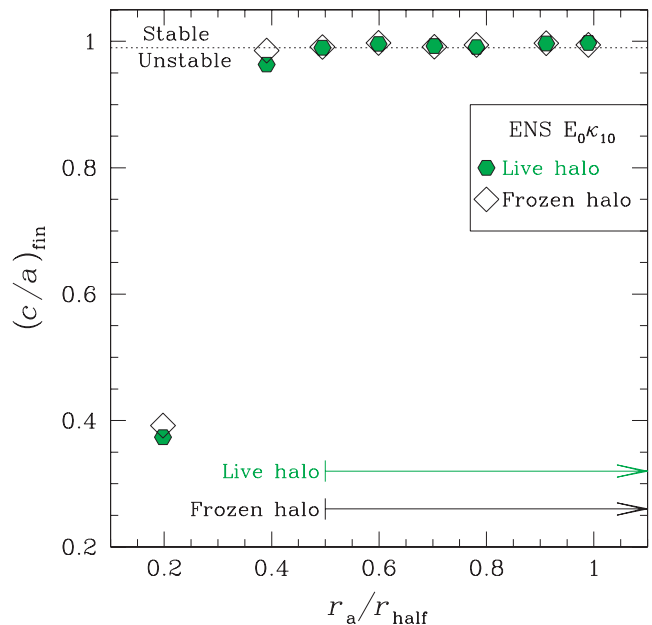

Figure 4. Final axial ratio $(c/a)_{fin}$ as a function of the initial anisotropy radius normalized to the half-mass radius for the ENSs with $\gamma = 0$ and $\kappa = 10$ when the DM halo is live (hexagons) and frozen (squares). The range of r_a/r_{half} corresponding to stable models (indicated by the arrows) is the same in the two cases.

parameter ξ_s) for stability are the same in the two cases. These results suggest that our conclusion that MOND models are substantially more subject to radial-orbit instability than ENSs should be robust, at least if the DM haloes are almost isotropic. Though the assumption of the isotropy of the haloes is not necessarily justified, given that the anisotropy of DM distributions is hard to constrain, it is clear that an isotropic halo can be always be invoked, in the context of Newtonian gravity, to stabilize an otherwise unstable strongly radially-anisotropic stellar system, while this freedom is not allowed in the context of MOND.

4 DISCUSSION AND CONCLUSIONS

To some extent, the MOND and DM interpretations of the kinematics of galaxies can be considered degenerate, that is, several observational features can be satisfactorily reproduced in both paradigms. This raises interesting questions about possible tests to discriminate between MOND and Newtonian gravity with the DM. Fortunately, it is now well established that some important dynamical processes *are* different, even in systems in which the total gravitational potentials are identical. Examples are dynamical friction and two-body relaxation.

In this work, we explored whether radial-orbit instability acts differently in MOND and in Newtonian gravity (with and without the DM); in addition to the theoretical interest, this study can be useful to constrain the interpretation of the observed kinematics of stellar systems in the two cases. In particular, we have focused on the stability of OM radially-anisotropic spherical γ-models ($\gamma = 0$ and 1). We compared the results obtained for MOND models, ENSs and purely baryonic Newtonian systems, all with the same stellar density distribution. Overall, we found that MOND systems are more prone to radial-orbit instability than their ENSs, independent of the specific indicator (r_a or ξ) used to quantify the anisotropy. Compared to purely baryonic Newtonian systems

with the same density profile, however, MOND systems have a larger minimum anisotropy radius for stability r_{as}, but nevertheless a higher maximum global anisotropy parameter for stability, ξ_s, a consequence of the larger kinetic energy that can be stored in their outer regions. We speculate that ξ_s is larger in MOND systems than in Newtonian systems with no DM for the same reasons that phase mixing and violent relaxation are less efficient, that is, because the force between particles in deep-MOND decreases with the distance less strongly (qualitatively as $1/r$) than in Newtonian gravity, so being nearer to the special case of harmonic oscillator interparticle forces, when instabilities and energy exchanges are impossible

Observationally, these findings may be relevant to applications of MOND to pressure-supported systems, such as globular clusters, dwarf spheroidal and elliptical galaxies. For instance, the velocity dispersion profiles of globular clusters in the outer parts of the Milky Way can been used to test MOND. In the case of the globular cluster NGC 2419, strong OM radial anisotropy (r_a close to r_{ac}) might be required in order to bring the velocity dispersion profile predicted by MOND close to the profile inferred from the observed radial velocities of the cluster stars (Sollima & Nipoti 2010). A combination of the stability constraints discussed in this paper with new observations of the radial velocity of stars can make the kinematics of NGC 2419 a crucial test for MOND (Ibata et al., in preparation).

Another family of objects that are very interesting from the perspective of MOND is that of dwarf spheroidal galaxies, because their low surface brightness, combined with their measured velocity dispersion, leads to conclude that they must be DM dominated if Newtonian gravity holds. Angus (2008) studied the observed line-of-sight velocity dispersion profiles of Milky Way dwarf spheroidal galaxies, finding that in most cases the data can be reproduced in MOND, at least with somewhat ad hoc anisotropy profiles. This result should be reconsidered on the basis of the consistency and stability constraints discussed in this work.

The kinematics of elliptical galaxies have also been considered as a possible test for MOND (e.g. Sanders 2000). As for globular clusters and dwarf spheroidals, when trying to reproduce the kinematics of ellipticals, the anisotropy of the velocity distribution of the stars is one of the variables in the problem and it is important to constrain it as much as possible, along the lines described in this paper. For instance, consistency constraints (but not the more stringent stability constraints) on the anisotropy of stars are considered in the recent investigation by Cardone et al. (2011). Some authors (Tiret et al. 2007; Klypin & Prada 2009) used the observed kinematics of planetary nebulae or of the satellites around elliptical galaxies as a test for MOND, allowing for quite general anisotropy profiles for the satellite system. In this case, however, while some limits on the amount of radial anisotropy might come from the requirement of consistency, stability arguments do not necessarily lead to strong constraints as long as the considered tracers are not dynamically dominant.

REFERENCES

An J., 2011, MNRAS, doi:10.1111/j.1365-2966.2011.18324.x
An J. H., Evans N. W., 2006, ApJ, 642, 752
Angus G. W., 2008, MNRAS, 387, 1481
Barnes J., Hut P., Goodman J., 1986, ApJ, 300, 112
Barnes E. I., Lanzel P. A., Williams L. L. R., 2009, ApJ, 704, 372
Bekenstein J. D., Milgrom M., 1984, ApJ, 286, 7
Bertin G., Pegoraro F., Rubini F., Vesperini E., 1994, ApJ, 434, 94
Binney J., Tremaine S., 2008, Galactic Dynamics, 2nd edn. Princeton Univ. Press, Princeton, NJ
Brada R., Milgrom M., 1999, ApJ, 519, 590
Cardone V. F., Angus G., Diaferio A., Tortora C., Molinaro R., 2011, MNRAS, doi:10.1111/j.1365-2966.2010.18081.x
Christodoulou D. M., 1991, ApJ, 372, 471
Ciotti L., 1996, ApJ, 471, 68
Ciotti L., 1999, ApJ, 520, 574
Ciotti L., Binney J., 2004, MNRAS, 351, 285
Ciotti L., Morganti L., 2009, MNRAS, 393, 179
Ciotti L., Morganti L., 2010a, MNRAS, 401, 1091
Ciotti L., Morganti L., 2010b, MNRAS, 408, 1070
Ciotti L., Pellegrini S., 1992, MNRAS, 255, 561
Ciotti L., Londrillo P., Nipoti C., 2006, ApJ, 640, 741
Ciotti L., Nipoti C., Londrillo P., 2007, in Bertin G., Pozzoli R., Romé M., Sreenivasan K. R., eds, Collective Phenomena in Macroscopic Systems. World Scientific, Singapore, p. 177
Ciotti L., Morganti L., de Zeeuw P. T., 2009, MNRAS, 393, 491
Dehnen W., 1993, MNRAS, 265, 250
Dejonghe H., Merritt D., 1988, ApJ, 328, 93
Di Cintio P., Ciotti L., 2011, preprint (arXiv:1103.5436)
Fridman A. M., Polyachenko V. L., 1984, Physics of Gravitating Systems. Springer, New York
Henon M., 1973, A&A, 24, 229
Hernquist L., 1990, ApJ, 356, 359
Hjorth J., 1994, ApJ, 424, 106
Klypin A., Prada F., 2009, ApJ, 690, 1488
Londrillo P., Nipoti C., 2009, Mem. Soc. Astron. Ital. Suppl., 13, 89
Londrillo P., Nipoti C., Ciotti L., 2003, Mem. Soc. Astron. Ital. Suppl., 1, 18
Lynden Bell D., Lynden Bell R. M., 1999, Proc. R. Soc. A, 455, 475
May A., Binney J., 1986, MNRAS, 221, 13P
Merritt D., 1985, AJ, 90, 102
Merritt D., Aguilar L. A., 1985, MNRAS, 217, 787
Meza A., Zamorano N., 1997, ApJ, 490, 136
Meza A., Zamorano N., 1998, in Zaritsky D., ed., ASP Conf. Ser. Vol. 136, Stability of Elliptical Galaxies with Dark Halos. Astron. Soc. Pac., San Francisco, p. 400
Milgrom M., 1983, ApJ, 270, 365
Milgrom M., 1986, ApJ, 306, 9
Milgrom M., 1989, ApJ, 338, 121
Milgrom M., 2001, MNRAS, 326, 1261
Milgrom M., 2010, MNRAS, 403, 886
Nipoti C., Londrillo P., Ciotti L., 2002, MNRAS, 332, 901
Nipoti C., Londrillo P., Ciotti L., 2003, MNRAS, 342, 501
Nipoti C., Londrillo P., Ciotti L., 2007a, ApJ, 660, 256
Nipoti C., Londrillo P., Zhao H. S., Ciotti L., 2007b, MNRAS, 379, 597
Nipoti C., Londrillo P., Ciotti L., 2007c, MNRAS, 381, L104
Nipoti C., Ciotti L., Binney J., Londrillo P., 2008, MNRAS, 386, 2194
Osipkov L. P., 1979, Soviet Astron. Lett., 5, 42
Ostriker J. P., Peebles P. J. E., 1973, ApJ, 186, 467
Palmer P. L., Papaloizou J., 1987, MNRAS, 224, 1043
Polyachenko V. L., 1987, in de Zeeuw T., ed., Proc. IAU Symp. 127, Stability of Elliptical Galaxies – Theoretical Aspects. Reidel, Dordrecht, p. 301
Polyachenko V. L., Shukhman I. G., 1981, Soviet Astron., 25, 533
Saha P., 1991, MNRAS, 248, 494
Sanders R. H., 2000, MNRAS, 313, 767

Sanders R. H., McGaugh S. S., 2002, ARA&A, 40, 263
Sanders R. H., Noordermeer E., 2007, MNRAS, 379, 702
Sollima A., Nipoti C., 2010, MNRAS, 401, 131
Stiavelli M., Sparke L. S., 1991, ApJ, 382, 466
Swaters R. A., Sanders R. H., McGaugh S. S., 2010, ApJ, 718, 380
Tiret O., Combes F., 2007, A&A, 464, 517
Tiret O., Combes F., Angus G. W., Famaey B., Zhao H. S., 2007, A&A, 476, L1

Tremaine S., Richstone D. O., Byun Y. I., Dressler A., Faber S. M., Grillmair C., Kormendy J., Lauer T. R., 1994, AJ, 107, 634
Trenti M., Bertin G., 2006, ApJ, 637, 717
Van Hese E., Baes M., Dejonghe H., 2011, ApJ, 726, 80
Weinberg M. D., 1991, ApJ, 368, 66

This paper has been typeset from a TEX/LATEX file prepared by the author.